


RESEARCH ARTICLE | DECEMBER 05 2023

Facile deposition of $\text{Cu}_2\text{O}/\text{ZnO}$ heterostructures on carbon fibers by plasma–liquid interaction toward enhanced piezoelectric performance

Special Collection: [Carbon-based Materials for Energy Conversion and Storage](#)

Ziyang Zhong; Hao Huang ; Ming Gao  ; Quanzhi Zhang ; Yun-Ge Zhang; Zilan Xiong ; Yifan Huang 



Appl. Phys. Lett. 123, 233903 (2023)

<https://doi.org/10.1063/5.0177759>

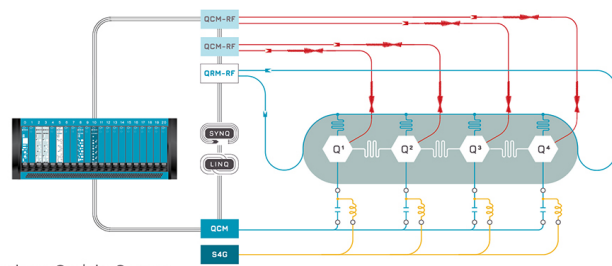


CrossMark



Integrates all
Instrumentation + Software
for Control and Readout of

Superconducting Qubits
NV-Centers
Spin Qubits



Superconducting Qubit Setup

[find out more >](#)

Facile deposition of Cu₂O/ZnO heterostructures on carbon fibers by plasma–liquid interaction toward enhanced piezoelectric performance

Cite as: Appl. Phys. Lett. **123**, 233903 (2023); doi: 10.1063/5.0177759

Submitted: 24 September 2023 · Accepted: 21 November 2023 ·

Published Online: 5 December 2023



View Online



Export Citation



CrossMark

Ziyang Zhong,^{1,2} Hao Huang,¹ Ming Gao,^{1,2,a)} Quanzhi Zhang,³ Yun-Ge Zhang,¹ Zilan Xiong,⁴ and Yifan Huang^{1,2}

AFFILIATIONS

¹Shenzhen Institute of Advanced Technology, Chinese Academy of Sciences, Shenzhen 518055, China

²University of Chinese Academy of Sciences, Beijing 100049, China

³School of Physics, Dalian University of Technology, Dalian 116024, China

⁴State Key Laboratory of Advanced Electromagnetic Technology, Huazhong University of Science and Technology, Wuhan 430074, China

Note: This paper is part of the APL Special Collection on Carbon-based Materials for Energy Conversion and Storage.

a) Author to whom correspondence should be addressed: ming.gao@siat.ac.cn

ABSTRACT

In this study, a facile and effective approach for the preparation of Cu₂O/ZnO heterostructures on flexible carbon materials to enhance the piezoelectric performance is reported. The Cu₂O/ZnO heterostructures are deposited directly on carbon fibers (CFs) by a two-step method using plasma–liquid interaction strategy. The Cu₂O microparticles are first deposited on the surface of CFs, and then, the ZnO nanostructures are grown on the surface of Cu₂O microparticles and CFs. The as-prepared CFs show an improved piezoelectric response of $d_{33} = 7.95$ pm/V compared to intrinsic CFs ($d_{33} = 2.64$ pm/V), which is based on the nano-heterostructures principle. This work demonstrates a simple and feasible approach to prepare flexible carbon materials with enhanced piezoelectric performance, which may provide an ecologically friendly option for the deposition of semiconductor heterostructures.

Published under an exclusive license by AIP Publishing. <https://doi.org/10.1063/5.0177759>

With the development of wearable and flexible electronics, semiconductor heterostructures on flexible carbon fibers (CFs) have attracted considerable attention for optoelectronic applications.^{1,2} Typically, the design of carbon materials based semiconductor heterostructures can be employed as a promising piezoelectric material for converting mechanical energy into electricity.³ Versatile semiconductor heterostructures have been emerged as a result of continuous research, and significant effort has been devoted to enhance the piezoelectric performance. Among various metal oxide heterostructures, Cu₂O/ZnO heterostructures are considered potentially interesting candidates due to their diverse characteristics such as environmentally friendly, natural p–n characteristics, and low-cost.^{4,5} They can increase the piezoelectric potential significantly by suppressing the screening effect.⁶

Up to now, there are varieties of techniques available to prepare the Cu₂O/ZnO heterostructures, such as hydrothermal reaction, photodeposition, and so on.^{7–9} However, most of the available reports

have used two different methods to fabricate the ZnO and Cu₂O layers. For example, the heterostructures can be prepared by hydrothermal method and magnetron sputtering.¹⁰ Despite that great achievements on this strategy have been made, there is still an unmet need for more effective and less toxic. It is expected to construct heterostructures by simply using single fabrication technique. Recently, ZnO and Cu₂O heterojunctions have been deposited by the co-sputtering system using ZnO and Cu targets.¹¹ Unfortunately, limited reports are available for the deposition Cu₂O/ZnO heterostructures on CFs by this simple strategy. Only ZnO@TiO₂ array heterostructures and MoS₂/CoS heterostructures on CFs have been fabricated by atomic layer deposition and hydrothermal procedure, respectively.^{12,13}

Compared to the deposition process with high vacuum and high temperature, atmospheric pressure plasma deposition has been attracted much more attention due to the advantages of low synthesis temperature and highly cost effective.^{14,15} Nevertheless, the reports on the Cu₂O/ZnO heterostructures on CFs are still limited. Thanks to the

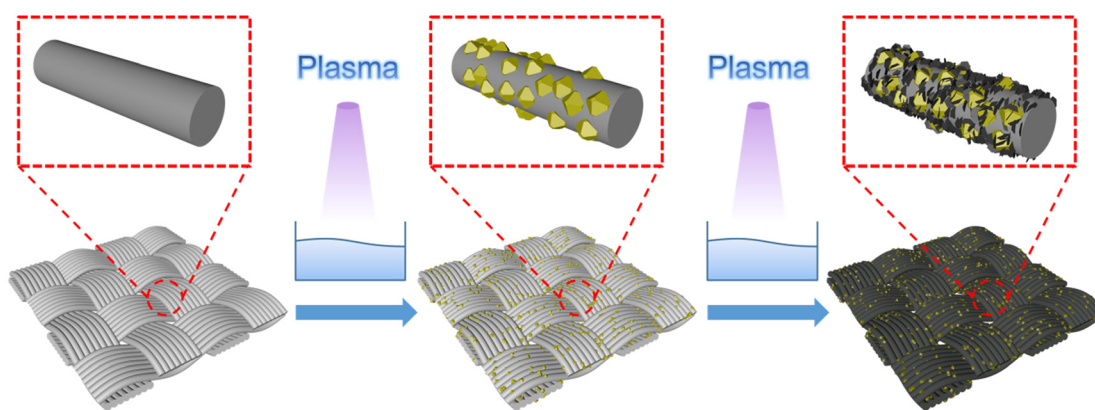


FIG. 1. Schematic diagram of the fabrication process of $\text{Cu}_2\text{O}/\text{ZnO}$ heterostructures.

great versatility of the plasma, plasma–liquid interaction is emerging as a highly efficient method for preparing composite materials with different compositions.^{16,17} The plasma–liquid interaction can achieve high reaction yields with the potential of more selective chemistry at atmospheric pressure and room temperature.¹⁸ Inspired by these previous reports, this study brings a way of fabricating $\text{Cu}_2\text{O}/\text{ZnO}$ heterostructures on CFs by using plasma–liquid interaction. Cu_2O microparticles and ZnO nanostructures have been deposited on CFs by a two-step process in a single plasma–liquid configuration. The piezoelectric performance of the CFs can be significantly enhanced with the heterostructures.

Here, a two-step aqueous solution method is applied to deposit $\text{Cu}_2\text{O}/\text{ZnO}$ heterostructures on CFs by plasma–liquid interaction. In the first step, the CFs with the desired size of $1.5 \times 2.5 \text{ cm}^2$ are successively cleaned in ethanol for 3 min and then dried in an oven at 80°C . The cleaned fibers are connected to the negative electrode of the power supply and immersed in the CuSO_4 solution (22 g/l). A stainless steel needle was fixed 2 mm above the liquid level and connected to the positive electrode of the power supply. The applied voltage is fixed at 1.5 kV, and the stable discharge of the plasma can be obtained. The Cu_2O microparticles have been deposited on the as-cleaned fibers by the plasma discharge generated between the needle and the liquid surface for 30 min. Subsequently, the as-prepared fibers are washed with ultrapure water, and then, the fibers are connected to the negative electrode again and immersed in the ZnSO_4 solution (40 g/l). The plasma discharge process is carried out via the same procedure. After discharge for 30 min, the ZnO nanostructures have been deposited, and the as-prepared fibers are washed and dried. Then, the $\text{Cu}_2\text{O}/\text{ZnO}$ heterostructures on CFs are prepared.

Scanning electron microscopy (SEM, Carl Zeiss Supra 55) was used to observe the surface morphology of the samples. Energy dispersive spectroscopy (EDS, Carl Zeiss X80) was applied to confirm the content of the samples. X-ray photoelectron spectroscopy (XPS, Thermo Fisher ESCALAB 250 Xi) was used to analyze the chemical composition of the samples. The piezoelectric response of the samples was measured by piezoresponse force microscopy (PFM). A conductive silver paste was coated onto the sample disk, and the sample was submerged horizontally into the paste. The tip of a silicon probe was placed on top of the samples with an AC voltage of 0–5 V applied. Data sampling was performed using a continuous read mode, which

allowed the voltage to vary continuously with time at a fixed frequency, and recorded 100 data points in the range of 0–5 V.

The schematic diagram of the whole fabrication process is shown in Fig. 1, including Cu_2O microparticles deposition and $\text{Cu}_2\text{O}/\text{ZnO}$ heterostructure construction. When the voltage applies to the electrodes, the cationic species (Cu^{2+}) in the solution will move toward the negative electrode (CFs) by the electric force based on the applied electrical polarity. When the plasma is in contact with the liquid, plasma-injected solvated electrons can be produced in the liquid phase.¹⁹ In addition to the electron, the plasma–liquid interaction will lead to the decomposition and ionization of water molecule, producing various active species in a liquid phase, such as hydrogen atom and OH radical.²⁰ These reactive species quickly change to other long-lived species, such as H_2 , OH^- , and so on, due to their high activity.²¹ These plasma-induced liquid species can be responsible for the reduction chemistry.²² Therefore, the possible reactions are described as follows:

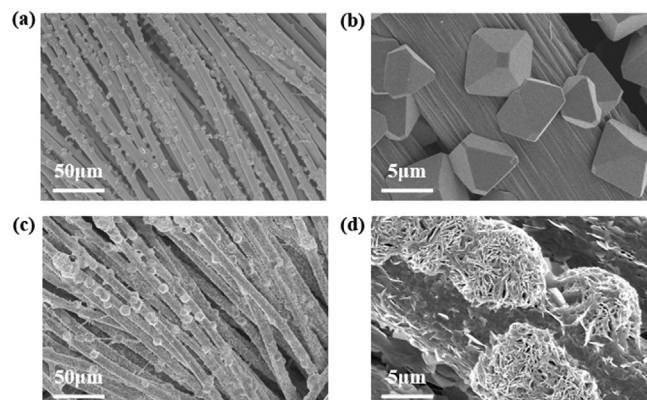


FIG. 2. SEM images of (a) Cu_2O microparticles and (c) $\text{Cu}_2\text{O}/\text{ZnO}$ heterostructures on the surface of CFs. (b) and (d) Higher magnification of the respective samples.

After the deposition of Cu_2O microparticles, the ZnSO_4 solution will be in place for the deposition. Similarly, Zn^{2+} ions also move toward the CFs electrode by the electric field, and the ions will bind to OH^- to initiate the growth of ZnO .²³ The plasma-liquid interaction can produce lots of active radical, leading to the formation of ZnO nanostructures on the surface of CFs. These main reactions can be described as follows:

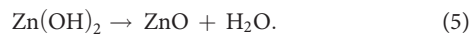


Figure 2 depicts the SEM images of the samples, including Cu_2O microparticles and $\text{Cu}_2\text{O}/\text{ZnO}$ heterostructures. Compared to the pristine carbon fiber with clear surface (Fig. S1 of the supplementary

material), it can be observed from Fig. 2(a) that Cu_2O microparticles are uniformly distributed on the surface of CFs. Figure 2(b) shows the high-magnifications of a single fiber with the monodisperse Cu_2O microparticles, and the average diameters of the microparticles are about $5\ \mu\text{m}$. The microparticles exhibit cubic and tetradecahedral shape in a good manner. From Fig. 2(b), it can be seen that ZnO nanostructures are also grown densely on the surface of CFs and Cu_2O microparticles. According to the high magnification image from Fig. 2(d), it shows that the ZnO nanostructures cover the fiber entirely, and the nanostructures grow all over the Cu_2O microparticles surface. Moreover, the nanostructures on the Cu_2O microparticles seem to be more compact, due to the large gap in lattice parameters between ZnO and Cu_2O .²⁴ It can be concluded that the $\text{Cu}_2\text{O}/\text{ZnO}$ heterostructures are uniformly synthesized on the CFs surface.

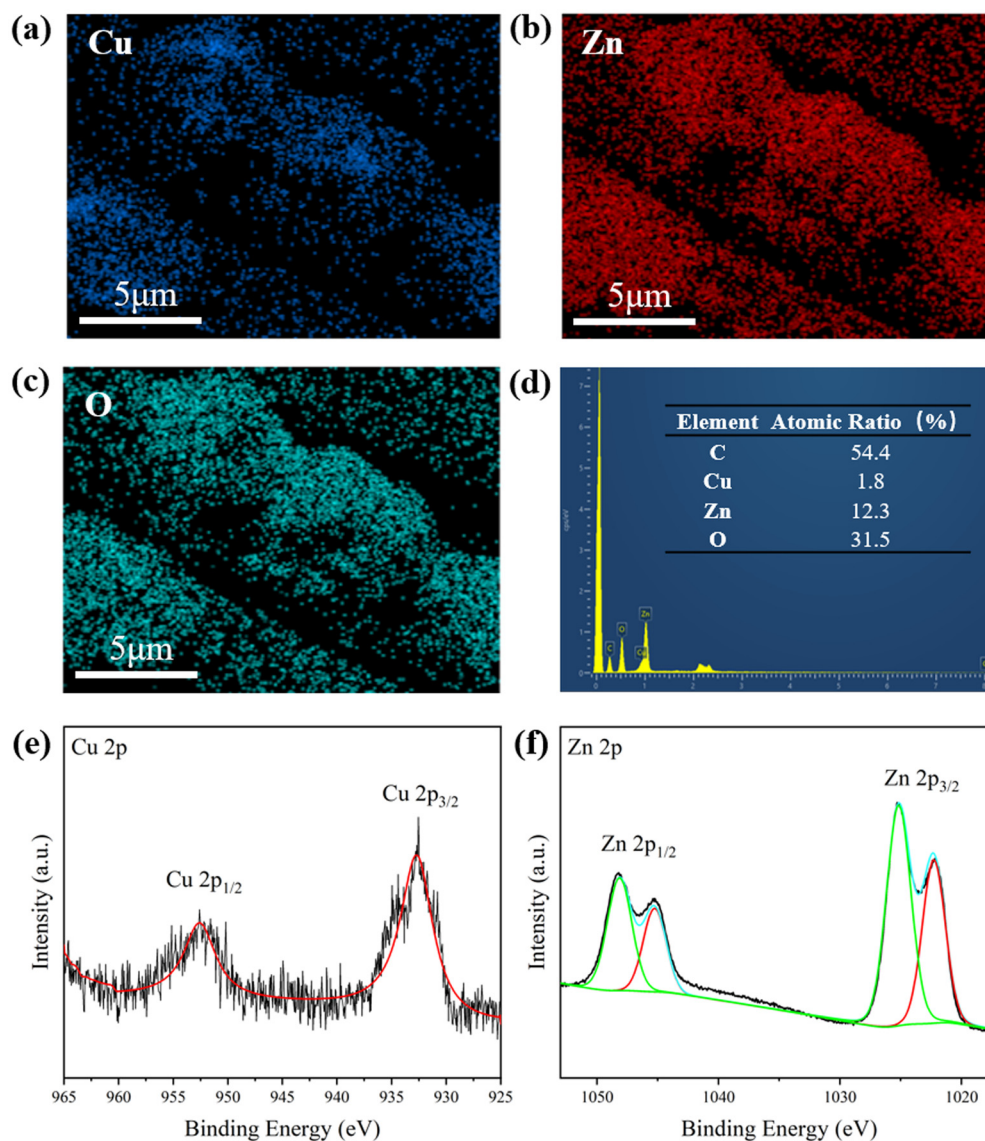


FIG. 3. EDS analysis (a)–(d) and XPS spectra (e) and (f) of $\text{Cu}_2\text{O}/\text{ZnO}$ heterostructures on the surface of CFs.

The EDS is also characterized for the samples, and the mapping of the distribution of the atoms is illustrated in Fig. 3. As shown in Figs. 3(a)–3(c), the elements Cu (blue), Zn (red), and O (green) are obtained. Compared to the individual elemental in the Cu₂O microparticles (Fig. S2 of the supplementary material), it also can be seen that Zn and O elements are distributed throughout the fiber, which is consistent with the SEM images. In addition, previous works have shown that the regions of interfacial contact between the two oxides in the formation of the CuO/ZnO heterostructure can be observed.²⁵ Therefore, the EDS clearly reveals the geometry in the Cu₂O/ZnO heterostructures.

XPS is further used to determine the chemical state of the Cu element and the Zn element in the as-synthesized nanostructures. In the high-resolution Cu 2p spectrum [Fig. 3(e)], the peaks of Cu 2p_{1/2} (952.55 eV) and Cu 2p_{3/2} (932.75 eV) clearly indicate that the deposited layer is Cu₂O rather than Cu or CuO.^{26,27} In comparison with the spectrum of the Cu₂O microparticles on the surface of CFs (Fig. S3 of the supplementary material), these peaks are slightly shifted (0.5 eV) to high binding energy, due to an interaction between the Cu₂O and ZnO. For the high-resolution Zn 2p spectrum, four different peaks appear, owing to the ZnO nanostructures grown on the surface of CFs and Cu₂O microparticles. The peaks of Zn 2p_{1/2} (1044.10 eV) and Zn 2p_{3/2} (1020.95 eV) correspond to the ZnO nanostructures on the surface of CFs, which agrees well with previous studies.²⁸ Since it is known that Cu₂O–ZnO heterostructures can have a significant effect on the energy band shift of ZnO, the peaks at 1047.05 and 1023.82 eV shifted to higher energy levels can be assigned to the ZnO nanostructures on Cu₂O microparticles surface.^{29,30} Moreover, the shifted energy is approximately 2.90 eV, which fits the similar reports well. In a previous

study, Yang *et al.* demonstrated that the type of Cu₂O–ZnO hetero-junction is related to its growth order, leading to different valence band offsets (VBO).³¹ This difference in VBO might be attributed to the different arrangement of atoms at the heterogeneous interface resulting from the varied growth order. The corresponding valence band offsets could be calculated as follows:

$$\Delta E_V^i = \left(E_{\text{Cu}_2\text{O}}^{\text{Cu}_2\text{O}}(i) - E_{\text{Zn}_2\text{O}}^{\text{Zn}_2\text{O}}(i) \right) + \left(E_{\text{Cu}_2\text{O}}^{\text{Cu}_2\text{O}} - E_{\text{VBM}}^{\text{Cu}_2\text{O}} \right) - \left(E_{\text{Zn}_2\text{O}}^{\text{Zn}_2\text{O}} - E_{\text{VBM}}^{\text{Zn}_2\text{O}} \right). \quad (6)$$

According to the above equation, the VBO of the Cu₂O–ZnO heterojunction (ZnO grown after Cu₂O) is calculated to be 2.91 eV. Thus, the above-mentioned results indicate that the Cu₂O/ZnO heterostructures have been deposited on the surface of CFs. Moreover, it is shown that the resulted heterostructures has been prepared without other harmful products, which is due to the deposition process does not need any additional chemicals. The high quality of the heterostructures on the surface of CFs will provide the basis for the next piezoelectric performance tests.

PFM has emerged as advanced scanning probe tools used to detect the piezoelectric properties of materials at the nanoscale.^{32,33} Figure 4 shows the piezoelectric properties of the as-prepared sample. In the continuous DC mode (–5 to +5 V), the phase-voltage hysteresis loop of the sample in Fig. 4(a) exhibits a high residual polarization intensity with and a narrow width, which is similar to the behavior of the single crystal. This result indicates that the sample can exhibit polarization rotation behavior with a phase angle change close to 180°. ³⁴ The amplitude–voltage butterfly curve depicts a good linear

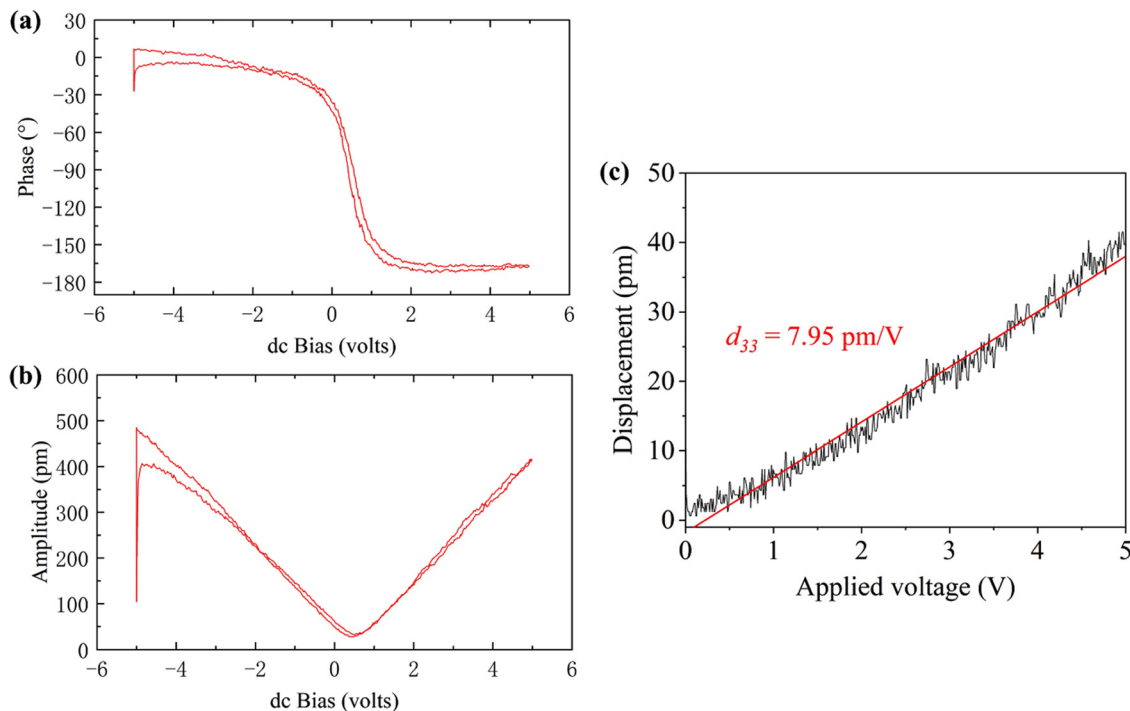


FIG. 4. Piezoresponse hysteresis loop of the sample: (a) phase, (b) amplitude, and (c) d_{33} .

relationship between the applied voltage and the sample amplitude, indicating that the sample has the partial piezoelectric response with low hysteresis.³⁵ To accurately calculate the piezoelectric constant d_{33} of the samples, the amplitudes are measured continuously in the AC mode (0 to +5 V). From the slope of the linear fit of amplitude vs voltage, the d_{33} value of the sample is determined to be 7.95 pm/V, while the original carbon fiber had a d_{33} value of 2.64 pm/V (Fig. S4 of the supplementary material). Based on the above-mentioned results, it can be concluded that the additional Cu₂O microparticles may effectively reduce the potential screening from intrinsic free electron carriers in ZnO, resulting in an enhanced piezoelectric response.³⁶

In summary, a plasma-liquid interaction strategy has been applied for the deposition of Cu₂O/ZnO heterostructures on CFs toward to enhanced the piezoelectric performance. The preparation of Cu₂O/ZnO heterostructures is confirmed with the help of microscopic morphology and chemical analysis, and the heterostructures exhibit high residual polarization intensity with a narrow width and partial piezoelectric response with low hysteresis. By adding a layer of Cu₂O microparticles between ZnO nanostructures and surface of CFs, the piezoelectric constant d_{33} of the CFs is enhanced from 2.64 to 7.95 pm/V. This study brings a simple and feasible strategy to fabricate semiconductor heterostructures on flexible CFs, which can potentially provide more environmentally friendly manufacturing options. Moreover, the integration of semiconductor heterostructures in flexible CFs has been exhibited in this study, which can be considered as alternative carbon materials for flexible optoelectronic applications.

See the supplementary material for the SEM images of CFs, EDS analysis of Cu₂O microparticles, Cu 2p XPS spectra of Cu₂O microparticles, and piezoelectric performance of CFs.

This work was funded by the National Natural Science Foundation of China (No. 62001459) and the Natural Science Foundation of Guangdong Province (No. 2022A1515011959).

AUTHOR DECLARATIONS

Conflict of Interest

The authors have no conflicts to disclose.

Author Contributions

Ziyang Zhong: Conceptualization (equal); Data curation (equal); Investigation (equal); Writing – original draft (equal). **Hao Huang:** Formal analysis (equal); Methodology (equal). **Ming Gao:** Conceptualization (equal); Investigation (equal); Supervision (equal); Writing – review & editing (equal). **Quanzhi Zhang:** Investigation (equal). **Yunge Zhang:** Funding acquisition (equal). **Zilan Xiong:** Investigation (equal); Writing – review & editing (equal). **Yifan Huang:** Supervision (equal); Validation (equal).

DATA AVAILABILITY

The data that support the findings of this study are available within the article.

REFERENCES

- Y. Li, J. Zhang, Q. Chen, X. Xia, and M. Chen, *Adv. Mater.* **33**(27), 2100855 (2021).
- Y. J. Hong, R. K. Saroj, W. I. Park, and G. C. Yi, *APL Mater.* **9**, 060907 (2021).
- X. Zhou, B. Shen, A. Lyubartsev, J. Zhai, and N. Hedin, *Nano Energy* **96**, 107141 (2022).
- T. Ozdal and H. Kavak, *Superlattices Microstruct.* **146**, 106679 (2020).
- B. H. Park, H. Park, T. Kim, S. J. Yoon, Y. Kim, N. Son, and M. Kang, *Int. J. Hydrogen Energy* **46**(77), 38319 (2021).
- Q. Wang, Y. Qiu, D. Yang, B. Li, X. Zhang, Y. Tang, and L. Hu, *Appl. Phys. Lett.* **113**, 053901 (2018).
- J. Xu, S. Song, J. Li, Y. Ji, Z. Li, D. Fu, Z. Zhong, G. Xu, and F. Su, *J. Catal.* **419**, 99 (2023).
- R. R. Kumar, W. C. Yu, T. Murugesan, P. C. Chen, A. Ranjan, M. Y. Lu, and H. N. Lin, *J. Alloys Compd.* **952**, 169984 (2023).
- X. Fei, D. Jiang, and M. Zhao, *J. Lumin.* **254**, 119477 (2023).
- S. Zhong, D. Xiong, B. Zhang, X. Yang, T. Yang, G. Tian, H. Zhang, W. Yang, and W. Deng, *ACS Photonics* **9**(1), 268 (2022).
- T. T. Nguyen, O. C. Emeka, N. Kumar, P. Bhatnagar, and J. Kim, *Mater. Today Commun.* **34**, 105205 (2023).
- L. Wang, X. Gu, L. Zhao, B. Wang, C. Jia, J. Xu, Y. Zhao, and J. Zhang, *Electrochim. Acta* **295**, 107 (2019).
- F. Xue, F. Fan, Z. Zhu, Z. Zhang, Y. Gu, and Q. Li, *Nanoscale* **15**, 6822 (2023).
- S. Banerjee, E. Adhikari, P. Sapkota, A. Sebastian, and S. Ptasinaka, *Materials* **13**(13), 2931 (2020).
- C. Xiong, Y. Wang, L. Lin, M. Gao, Y. Huang, and P. K. Chu, *Surf. Interfaces* **37**, 102758 (2023).
- F. Rezaei, P. Vanraes, A. Nikiforov, R. Morent, and N. D. Geyter, *Materials* **12**(17), 2751 (2019).
- Z. Zhong, C. Wang, R. Han, M. Gao, Y. Huang, and S. Ramakrishna, *Compos. Commun.* **38**, 101495 (2023).
- P. J. Bruggeman, R. R. Frontiera, U. R. Kortshagen, M. J. Kushner, S. Linic, G. C. Schatz, H. Andaraarachchi, S. Exarhos, L. O. Jones, C. M. Mueller, C. C. Rich, C. Xu, Y. Yue, and Y. Zhang, *J. Appl. Phys.* **129**(20), 200902 (2021).
- P. Rumbach and D. B. Go, *Top. Catal.* **60**, 799 (2017).
- D. A. Shutov, A. V. Sungurova, A. Choukourov, and V. V. Rybkin, *Plasma Chem. Plasma Process.* **36**, 1253 (2016).
- J. Liu, B. He, X. Wang, Q. Chen, and G. Yue, *Eur. Phys. J. D* **73**, 11 (2019).
- T. Kaneko and R. Hatakeyama, *Jpn. J. Appl. Phys., Part 1* **57**, 0102A6 (2018).
- T. Iqbal, A. Aziz, M. A. Khan, S. Andleeb, H. Mahmood, A. A. Khan, R. Khan, and M. Shafique, *Mater. Sci. Eng., B* **228**, 153 (2018).
- L. Cheng, G. Wu, D. Ruan, H. Wu, and A. Liu, *J. Mater. Sci.* **58**, 186 (2023).
- M. C. Oliveira, V. S. Fonseca, N. F. Andrade Neto, R. A. P. Ribeiro, E. Longo, S. R. de Lazaro, F. V. Motta, and M. R. D. Bomio, *Ceram. Int.* **46**(7), 9446 (2020).
- D. Xiong, W. Deng, G. Tian, Y. Gao, X. Chu, C. Yan, L. Jin, Y. Su, W. Yan, and W. Yang, *Nanoscale* **11**, 3021 (2019).
- H. Zhang, G. Tian, D. Xiong, T. Yang, S. Zhong, L. Jin, B. Lan, L. Deng, S. Wang, Y. Sun, W. Yang, and W. Deng, *ACS Appl. Mater. Interfaces* **14**(25), 29061 (2022).
- N. Celebi and K. Salimi, *J. Colloid Interface Sci.* **605**, 23 (2022).
- Y. Sun, X. Wang, Q. Fu, and C. Pan, *Appl. Surf. Sci.* **564**, 150379 (2021).
- N. J. Karazmoudeh, M. Soltanieh, and M. Hasheminiasari, *J. Alloys Compd.* **947**, 169564 (2023).
- M. Yang, L. Zhu, Y. Li, L. Cao, and Y. Guo, *J. Alloys Compd.* **578**, 143 (2013).
- Y. Calahorra, A. Datta, J. Farnelton, D. Kam, O. Shoseyov, and S. K. Narayan, *Nanoscale* **10**, 16812 (2018).
- H. Ursic and M. Sadl, *Appl. Phys. Lett.* **121**, 192905 (2022).
- J. Xiao, T. S. Herng, J. Ding, and K. Zeng, *J. Alloys Compd.* **709**, 535 (2017).
- M. C. Maldonado-Orozco, M. T. Ochoa-Lara, J. E. Sosa-Marquez, R. P. Talamantes-Soto, A. Hurtado-Macias, R. L. Anton, J. A. Gonzalez, J. T. Holguin-Momaca, S. F. Olive-Mendez, and F. Espinosa-Magana, *J. Am. Ceram. Soc.* **102**(5), 2800 (2019).
- Y. Nie, Y. Qiu, D. Yang, X. Zhang, and L. Hu, *J. Mater. Sci.* **30**, 9466 (2019).